

Appendix: Corrections for Anisotropically Averaged Hyperfine Splittings and Order Parameters from Pseudopowder Electron Paramagnetic Resonance (EPR) Line Shapes An Update for Slow-Motion Contributions to Lipid Spin Label Spectra from Membranes

Derek Marsh and Karl Schorn

In the first volume of this series (Berliner, 1976), consideration was given to corrections that must be made to extract order parameters from the EPR spectra of lipid spin labels in randomly oriented membrane dispersions (Gaffney, 1976; Griffith and Jost, 1976). A similar analysis leading to a somewhat different correction was also given previously by Hubbell and McConnell (1971). A hybrid of these results, depending on the range of order parameters studied ($0 \leq S_{app} < 0.45$ or 0.45

Derek Marsh and Karl Schorn • Max-Planck-Institut für biophysikalische Chemie, D-37108 Göttingen, Germany.

Biological Magnetic Resonance, Volume 14: Spin Labeling: The Next Millennium, edited by Berliner. Plenum Press, New York, 1998.

$\leq S_{app} \leq 1$) was given later by Marsh (1985), based on results of simulations presented by Griffith and Jost (1976). These corrections were widely used to analyze membrane EPR spectra from doxyl-labeled lipid chains, and these continue to be so. The purpose of this appendix is to update these corrections to account for components of lipid chain motion in fluid membranes that are now known to be in the slow regime of conventional nitroxide EPR spectroscopy (compare Freed, 1976; Schneider and Freed, 1989).

Restricted anisotropic rotation of spin-labeled lipid chain segments in fluid membranes is specified by an order tensor with principal element S_{zz} (relative to the membrane normal). This limited anisotropic reorientation results in the following principal elements of the partially motionally averaged hyperfine tensor (see, e.g., Seelig, 1976; Marsh and Horváth, 1989):

$$A_{\parallel} = a_o + (2/3)\Delta A \cdot S_{zz} \quad (1)$$

$$A_{\perp} = a_o - (1/3)\Delta A \cdot S_{zz} \quad (2)$$

where with a ^{14}N -hyperfine tensor $\mathbf{A} = (A_{xx}, A_{yy}, A_{zz})$, the isotropic hyperfine coupling constant is $a_o = (1/3)(A_{xx} + A_{yy} + A_{zz})$ and the maximum extent of the axial hyperfine anisotropy is $\Delta A = A_{zz} - 1/2(A_{xx} + A_{yy})$. Here it is assumed that the z -principal axis of the ^{14}N -hyperfine tensor is oriented parallel to the molecular axis, as for stereospecifically doxyl- or proxyl-labeled lipid chains. It is also assumed that the nonaxiality of the ^{14}N -hyperfine tensor is small, as is found experimentally, such that only the S_{zz} principal element of the ordering tensor is required to describe its anisotropic motional averaging.

For a powder pattern EPR line shape or a partially averaged EPR spectrum resulting from fast anisotropic reorientation in an unoriented membrane suspension, the splitting between the outer hyperfine extrema of the first-derivative spectrum $2A_{\text{max}}$ is rigorously equal to $2A_{\parallel}$ (Weil and Hecht, 1963; Hubbell and McConnell, 1971). However the effective splitting of the inner hyperfine extrema A_{min} is complicated by spectral overlap in this region of the (pseudo-)powder line shape. Previous corrections proposed to determine order parameters from randomly oriented samples related this effective inner splitting $2A_{\text{min}}$ to the true value of the hyperfine splitting given by $2A_{\perp}$ (Hubbell and McConnell, 1971; Griffith and Jost, 1976; Gaffney, 1976). These empirical corrections were based on the simulation of powder spectra corresponding to the motionally averaged hyperfine tensor $\mathbf{A}' = (A_{\perp}, A_{\perp}, A_{\parallel})$. These corrections therefore correspond to fast partial motional averaging of the hyperfine anisotropy. Unlike the situation in soap systems, which exhibit fast motional averaging and high order (Schindler and Seelig, 1971; Seelig, 1976), EPR spectra from chain-labeled lipids in fluid phospholipid membranes contain important features corresponding to motional components that are slow on the conventional nitroxide EPR time scale (Lange *et al.*, 1985; Moser *et al.*, 1989).

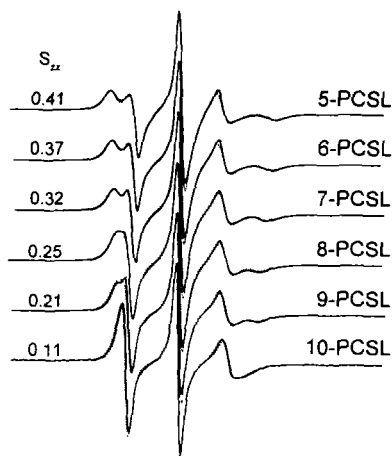


Figure 1. Experimental EPR spectra (*solid lines*) and simulations using the VAR model (*dotted lines*) for different positional isomers of the n-PCSL phosphatidylcholine spin labels in dimyristoyl phosphatidylcholine/dimyristoyl glycerol (58:42) mol/mol bilayers at 60°C. The order parameters S_{zz} used in the simulations are indicated in the figure. Total scan range = 100 G (Schorn and Marsh, 1996).

In the pseudopowder EPR spectra from spin-labeled lipids in fluid phospholipid bilayers or biological membranes, the low-field perpendicular peak is characteristically less deep than that of the central line (see Fig. 1); this feature is reversed in soap systems, and it cannot be reproduced by simulations based on fast motional narrowing theory (Schindler and Seelig, 1973; Seelig, 1976). Furthermore the high-field parallel peak is less deep than the overshoot feature from the high-field perpendicular peak (see experimental spectra in Fig. 1); this feature is not reproduced (for $S_{zz} \leq 0.7$) by previous simulations used to obtain corrections for calculating order parameters (see Griffith and Jost, 1976; Gaffney, 1976).

To account for slow-motional contributions with spin-labeled lipids in membranes, spectral simulations were made using the very anisotropic reorientation (VAR) model (see Meirovitch *et al.*, 1984). This is the very simplest of the slow motional models that emulates, although it does not describe exactly, anisotropic local ordering in macroscopically unoriented samples. Nevertheless it was found to be very successful in systematically representing spin label EPR spectra from a variety of different lipid spin labels in bilayer membranes over a wide range of temperature and membrane lipid compositions (Schorn and Marsh, 1996). Figure 1 shows representative simulations of experimental spectra from different positional isomers of the 1-acyl-2-(n-doxy)l-phosphatidylcholines (n-PCSL) in fluid lipid membranes. Unlike the fast-motional analysis, experimental spectra can be fitted with a high degree of precision by simulations using the VAR model. Further refinement of the model is not justified by the relatively low resolution obtained in experimental spectra from nonaligned membrane samples.

The EPR spectra were simulated for ^{14}N -nitroxide spin labels at a microwave frequency of 9.0 GHz for the full range of molecular order parameters. $S_{zz} = 0-1$

by using the VAR model (Schorn and Marsh, 1997). The spin Hamiltonian parameters used were $\mathbf{A} = (5.9 \text{ G}, 5.4 \text{ G}, 32.9 \text{ G})$ and $\mathbf{g} = (2.0076, 2.0072, 2.0021)$ (Schorn and Marsh, 1996). This \mathbf{g} -tensor differs slightly from single-crystal values for a doxyl nitroxide (Jost *et al.*, 1971) because it has reduced nonaxiality to account in part for some of the effects of rapid *trans-gauche* isomerism not explicitly included in the model. Dynamic parameters and intrinsic line widths were chosen to reproduce experimental spectra typical of n-PCSL spin labels in membranes (see Schorn and Marsh, 1996; compare Fig. 1). Splittings between the outer peaks ($2A_{\max}$) and between the inner peaks ($2A_{\min}$) in simulated spectra were measured to establish empirical corrections that must be made to obtain the true hyperfine splittings $2A_{\parallel}$ and $2A_{\perp}$, respectively, which are used to determine the order parameter S_{zz} from Eqs. (1) and (2).

Values of $2A_{\max}$ measured from the simulated spectra vary linearly with S_{zz} from $2A_{\max} \approx 2a_o$ for $S_{zz} = 0$ to $2A_{\max} \approx 2A_{zz}$ for $S_{zz} = 1$ (Schorn and Marsh, 1997), as would be predicted by Eq. (1) from motional narrowing theory. For spectra that contain contributions from slow motional components however, this is neither an evitable nor necessarily expected result. It arises from a balance of the effects parallel and perpendicular components of the diffusion tensor have on the outer spectral line positions. Although somewhat fortuitous, this simple result corresponds best to experimental spectra in this model (Schorn and Marsh, 1996; see Fig. 1); it has the advantage that the relationship $A_{\parallel} = A_{\max}$ normally used may be retained to a reasonable degree of approximation.

Values of the inner splittings $2A_{\min}$ obtained from the simulated spectra do not correspond to Eq. (2) nor to those obtained previously from fast motional narrowing simulations. The dependence of A_{\min} on the order parameter is linear, at least over the range $S_{zz} = 0.05\text{--}0.8$ (for values outside this range, the inner splitting is difficult to resolve). This leads to the following relation for the A_{\perp} motionally averaged tensor element (Schorn and Marsh, 1997):

$$A_{\perp} = A_{\min} + 1.29 \text{ G} - 1.75 \text{ G} \cdot S_{zz} \quad (3)$$

This correction is similar in form to that introduced previously from motional narrowing simulations (Gaffney, 1976) except that in the latter case, both numerical terms had a value of 1.4 G.

Finally, the order parameter may be expressed in terms of the experimentally accessible parameter $S_{app} = (A_{\max} - A_{\min})/\Delta A$ by using Eqs. (1)–(3) with $A_{\parallel} = A_{\max}$:

$$S_{zz} = 1.069 S_{app} - 0.051 \quad (4)$$

where $\Delta A = 27.2 \text{ G}$. This very simple form allows immediate estimation of S_{zz} by using values of A_{\max} and A_{\min} obtained from experimental spectra. If necessary a further correction may be applied to account for differences in spin label environ-

ment polarity by using the ratio of the isotropic hyperfine coupling constants (Hubbell and McConnell, 1979; Gaffney, 1976; Jost and Griffith, 1976). The hyperfine tensor used here to determine the corrections corresponds to a value of $a_o = 14.7$ G, which is reasonably close to the mean value for doxyl labels in the acyl chain regions of lipid membranes (Marsh and Watts, 1981).

Including the polarity correction, which corresponds to $a'_o = (1/3)(2A_{\perp} + A_{\parallel})$, gives rise to a quadratic equation for S_{zz} . The solution of this may be approximated by:

$$S_{zz} = \frac{1}{7} (A_{\max} + 2A_{\min}) - \sqrt{\left[\frac{1}{7} (A_{\max} + 2A_{\min})\right]^2 - 0.46(A_{\max} - A_{\min}) + 0.6} \quad (5)$$

where A_{\max} and A_{\min} are expressed in gauss. Values for the order parameter obtained in this way agree quite well with those obtained by direct simulations, such as are given in Fig. 1 (Schorn and Marsh, 1997). The method may therefore be used with experimental spectra to yield order parameters that closely approximate those obtained by spectral simulations using the VAR slow motional model.

REFERENCES

- Berliner, L. J., 1976, ed. *Spin Labeling. Theory and Applications* (Academic, New York).
- Freed, J. H., 1976, Theory of slow tumbling ESR spectra for nitroxides, in *Spin Labeling. Theory and Applications* (L. J. Berliner, ed.) (Academic, New York), p. 53.
- Gaffney, B. J., 1976, Practical considerations for the calculation for order parameters for fatty acid or phospholipid spin labels in membranes, in *Spin Labeling. Theory and Applications* (L. J. Berliner, ed.) (Academic, New York), p. 567.
- Griffith, O. H., and Jost, P. C., 1976, Lipid spin labels in biological membranes, in *Spin Labeling. Theory and Applications* (L. J. Berliner, ed.) (Academic, New York), p. 453.
- Hubbell, W. L., and McConnell, H. M., 1971, *J. Am. Chem. Soc.* **93**:314.
- Jost, P. C., Libertini, L. J., Hebert, V. C., and Griffith, O. H., 1971, *J. Mol. Biol.* **59**:77.
- Lange, A., Marsh, D., Wassmer, K.-H., Meier, P., and Kothe, G., 1985, *Biochemistry* **24**:4383.
- Marsh, D., 1985, ESR probes for structure and dynamics of membranes, in *Spectroscopy and the Dynamics of Molecular Biological Systems* (P. M. Bayley and R. E. Dale, eds.) (Academic, London), p. 209.
- Marsh, D., and Horváth, L. I., 1989, Spin-label studies of the structure and dynamics of lipids and proteins in membranes, in *Advanced EPR. Applications in Biology and Biochemistry* (A. J. Hoff, ed.) (Elsevier, Amsterdam), p. 707.
- Marsh, D., and Watts, A., 1981, ESR spin label studies of liposomes, in *Liposomes: from Physical Structure to Therapeutic Applications* (C. G. Knight, ed.) (Elsevier/North-Holland, Amsterdam), p. 139.
- Meirovitch, E., Nayeem, A., and Freed, J. H., 1984, *J. Phys. Chem.* **88**:3454.
- Moser, M., Marsh, D., Meier, P., Wassmer, K.-H., and Kothe, G., 1989, *Biophys. J.* **55**:111.
- Schindler H., and Seelig, J., 1973, *J. Chem. Phys.* **59**:1841.
- Schneider, D., and Freed, J. H., 1989, Calculating slow motional magnetic resonance spectra, a user's guide, in *Spin Labeling. Theory and Applications. Biological Magnetic Resonance*, vol. 8 (L. J. Berliner and J. Reuben, eds.) (Plenum, New York), p. 1.
- Schorn, K., and Marsh, D., 1996, *Chem. Phys. Lipids* **82**:7.

- Schorn, K., and Marsh, D., 1997, *Spectrochim. Acta A* **53**:2235.
- Seelig, J., 1976, Anisotropic motion in liquid crystalline structures, in *Spin Labeling. Theory and Applications* (L. J. Berliner, ed.) (Academic, New York), p. 373.
- Weil, J. A., and Hecht, H. G., 1963, *J. Chem. Phys.* **38**:281.

Contents Of The Previous Volume In This Series

SPIN LABELING: THEORY AND APPLICATIONS, VOLUME 8, (1989)

Chapter 1

Calculating Slow Motional Magnetic Resonance Spectra: A User's Guide

David J Schneider and Jack H. Freed

Chapter 2

Inhomogeneously Broadened Spin-Label Spectra

Barney Bales

Chapter 3

Saturation Transfer Spectroscopy of Spin Labels: Techniques and Interpretation of Spectra

M. A. Hemminga and P. A. de Jager

Chapter 4

Nitrogen-15 and Deuterium Substituted Spin Labels for Studies of Very Slow Rotational Motion

Albert H. Beth and Bruce H. Robinson

*Chapter 5***Experimental Methods in Spin-Label Spectral Analysis***Derek Marsh**Chapter 6***Electron–Electron Double Resonance***James S. Hyde and Jim B. Feix**Chapter 7***Resolved Electron–Electron Spin–Spin Splittings in EPR Spectra***Gareth R. Eaton and Sandra S. Eaton**Chapter 8***Spin-Label Oximetry***James S. Hyde and Witold K. Subczynski**Chapter 9***Chemistry of Spin-Labeled Amino Acids and Peptides: Some New Mono- and Bifunctionalized Nitroxide Free Radicals***Kálmán Hideg and Olga H. Hankovsky**Chapter 10***Nitroxide Radical Adducts in Biology: Chemistry, Applications, and Pitfalls***Carolyn Mottley and Ronald P. Mason**Chapter 11***Advantages of ^{15}N and Deuterium Spin Probes for Biomedical Electron Paramagnetic Resonance Investigations***Jane H. Park and Wolfgang E. Trommer*

Chapter 12

Magnetic Resonance Study of the Combining Site Structure of a Monoclonal Anti-Spin-Label Antibody

Jacob Anglister

Appendix

Approaches to the Chemical Synthesis of ^{15}N and Deuterium Substituted Spin Labels

Jane H. Park and Wolfgang E. Trommer

Index

Index

- Absorption, 90
Accessibility parameter, π , 69
ACET, 285, 302–304
Acetyl-carboxypeptidase, 238
Acetylsalicylic acid, 131, 132
Acetylcholine, 158, 172
Acetylcholinesterase
 enzymatic activity by ESR, 157
 modified by biradical disulfide, 159,
 160
Acetylthiocholine, 158
Activation energy, for molecular motion,
 356, 358, 360
Affinity, 298, 302, 320, 327–328
Alamethicin, 276
Alcohol dehydrogenase, 159–161
Alkylating nitroxide, 141, 147
Amidino nitroxide, 140
Amino nitroxide, 122, 140
3-Amino-PROXYL, 289, 290
4-Amino-TEMPO, 289, 290, 321, 323
Androstane spin label: *see* ASL
Angiotensin, spin-labeled, 141
Anisotropic rotational diffusion, 29
Anisotropy, hyperfine, 88
Apocytochrome *c*, 66
L-Arginine, 169, 171, 172
Arrhenius equation, 356, 358
(ASL) 3-doxyl-17 β -hydroxy-5 α -androstane,
 33, 88–90
A tensor, 341, 343
 isotropic value, 342
 principal value, 342
ATPase, Na⁺K⁺, 65
 vacuolar, 73
Azido nitroxide, 140
Bacteriorhodospin, 258–260
 α -helices, 259–260
Benzocaine, 131, 132
Bi(di)radical
 disulfide, 149
 exchange integral, 124, 150
 pH-sensitivity, 123, 125, 151
Bilayer membrane, 42, 73
Binomial distribution
 hyperfine multiplet, 6
 spinlabelpopulation, 11
Bioreduction, 373
Bovine serum albumin (BSA), 100–103
Broadening
 homogeneous, 53
 inhomogeneous, 6, 9, 14, 16, 54–55, 85, 90, 93
C-5 spin-labeled nucleoside (DUPDA), 285, 289
C-5 spin-labeled nucleoside (DUTA), 285, 288,
 289, 292
Capillary electrophoresis (CE), 296, 297, 334
 gas permeable, 94
Carbodiimide nitroxide, 140
 spin label, 77
Carbohydrate, 340, 351, 360
Carboxypeptidase A, 237, 243
 acetyl, 238
 mixed anhydride reaction intermediate of, 237
 spin-labeled substrates, 237

- Cavity
 in a glass, 356
 in a lattice, 345, 348, 350, 360
 microwave, 365
- Cecropins, 274–276
- Center-field ratio: *see* Line height ratio
- Chromium oxalate, paramagnetic relaxant, 69
- α -Chymotrypsin, 231–232, 243
 spin-labeled acylenzyme, 233, 236
 transition state inhibitor analog, 231
- Coat protein, M13, 71
- Comparative X- and W-band, EPR, 84–93
 bovine serum albumin, spin-labeled fatty acid binding, 100–102
 3-doxyl-17 β -hydroxy-5 α -androstane in O-xylene, 88–90
 doxyl stearic acid labels in phospholipid membranes, 97–100
 mixtures of phenyl-tert-butylnitron spin adducts, 90–93
 perdeuterated TEMPONE in toluene, 85–88
 small spin labels in phospholipid membranes, 95–97
 spin labeled phospholipids and proteins, 95–105
 spin labeled proteins
 immobilized labels, 102–104
 mobile labels, 104–105
- Correlation time, 29, 33, 35, 78, 305–306, 308, 315, 318–319, 330; *see also* Rotational correlation time
- Cryoenzymology, 230
- Crystallization, 348, 349
 crystals, 351
 formation, 354
 ice, 150
 melting, 349–352
- CSL (3-doxylcholestane) cholestane spin probe, 90
- CTPO, 33, 35–36, 379, 391; *see also* Spin label
- CW saturation, 255–256
 fast acting agents, 255
- Cysteine labeling, 152, 154–156, 159, 340–341, 356–357
- Cytochrome *c*, 66
- Cytochrome P-450 reductase, 159, 160
- DCAT, 286, 323, 324
- DCAVAP, 287, 295
- Degeneracy, 47
- Denaturation of FepA, 267–271
- Deoxygenation, CW HF EPR experiments, 93–95
- Desiccation tolerance, 340
- Deuterium hyperfine, 85
- Dextrin, 355
- DIACET, 286, 302
- Di-*t*-butylnitroxide, DTBN, 393
- Diagnostic intensity ratio, inhomogeneous broadening, 9, 14, 16
- Dielectric properties, 364
- Differential scanning calorimetry, 351–353, 360; *see also* DSC
- Diffusion, 349
 Brownian, 343
 rotational, 29, 77
 slow rotational, 77
 spin, 30, 35
 translational, 39–40, 63–65, 349
 water, 339
- Diffusion coefficient, translational, 39–40, 65
- 3,4-Dihydro-1,2-diazete, 1,2-dioxides, 168, 169
- 5,5-Dimethyl-1-pyrroline-N-oxide, 158
- 1,2-dipalmitoyl-*sn*-glycero-3-phosphatidylcholine (DPPC), 96, 97
- Diphtheria toxin, 273–274
- Dipolar interaction, 40, 72, 263, 265
 (END) electron nuclear dipolar, 35
 spin–spin interactions, 11
- Dipolar relaxation, 40, 72
- Dipole coupled nitroxide labels, 104
- Dipole–dipole interaction, 40, 72
- Distance measurements, 40, 73
- Dispersion, 90
- Distance measurements
 metal–nitroxide, 271–273
 nitroxide–nitroxide, 263–265
- Disulfide
 biradical, 149
 thiol–disulfide exchange, 149, 150
- Dithiocarbamates, 162, 167
- Dithioerythritol, 149, 160
- DMPC (1,2-dimyristoyl-*sn*-glycero-3-phosphocholine), 94–100
- DMPC-DSPC, 17–21
- DMPG spin label, 67–68
- B-DNA, 319, 323–324, 326
- Z-DNA, 323–325

- Domains
 disconnected, 19
 size, 11, 13
- Dosimetry, by EPR, 390
- Double cysteines, 263–265
 dipolar interactions, 263
 distance, 263
- Double labeling, 66
- Dough, 356
- 3-Doxyl-17 β -hydroxy-5 α -androstande (ASL),
 88, 89
- Doxyl stearic acid, 94, 95, 97–102
- DPPC (1,2-dipalmitoyl-*sn*-glycero-3-
 -phosphatidylcholine), 96–99
- DSPC spin label (DMPCSL), 17–20, 34, 68, 70
- DTBN, di-*t*-butylnitroxide, 393
- DUAP, 286, 294, 296, 301, 303, 310, 314–318,
 323, 326, 327, 330
- DUAT, 286, 293, 294, 301, 303
- DUAVAP, 287, 293, 294
- DUMPDA, 285, 289, 290, 298, 301, 321, 322
- DUMTA, 285, 290, 298, 303, 315, 316
- DUNTb, 285, 295–297
- DUPAT, 286, 293
- DUPDA, 5-[(1-Oxyl-2,2,5,5-tetramethyl-3-
 pyrrolidinyl)amino]-2'-deoxyuridine,
 285, 289
- DUTA, 5-[(1-Oxyl-2,2,6,6-tetramethyl-4-
 piperidinyl)amino]-2'-deoxyuridine,
 285, 288, 289, 292
- Drug delivery systems, measurement in tissues,
 377
- DSC, *see also* Differential scanning calorime-
 try
 molecular, 341, 354, 357, 359
- Electron–nuclear dipolar interaction (END), 35
- Electron relaxation, mechanism, 28
- Electrostatic potential
 human serum albumin, 147, 148, 159
 phospholipid membranes, 138, 139, 143–146
- Enaminoketone nitroxide, 128
- Endothelium-derived relaxing factor, EDRF,
 168
- ENDOR
 angle-selected, 190
 basis of torsion angle search, 187–188
 constraints, 209
¹H, 109
¹⁹F, 190, 216
 shift, 190
- Enzymatic synthesis
 digestion of spin-labeled oligomers, 292
 incorporation, 284, 292–294, 299
 spin labeled oligonucleotides, 284, 292,
 299
 spin labeling, 284, 292–295, 299
 template-independent enzymes, 292
 template dependent enzymes, 292
AmpliTaq DNA polymerase, 292, 294,
 295
 DNA polymerase I, 292
 DNA polymerase, Klenow fragment,
 293, 294
M. luteus DNA polymerase, 292, 294
 reverse transcriptase, 292
 T-4 DNA polymerase, 292, 293, 295
- Enzyme reaction intermediates, 229, 242
- EPR (electron paramagnetic resonance) or ESR
 (electron spin resonance)
 CW, 252, 255
 CW saturation, 255–257
 orientation selection in ENDOR, 187
 signal quantitation, 299–301
 specific activity, AEPR, 288, 289, 292,
 298–301
 spin echo, 271
- Exchange interaction, 42, 265, 256, 85, 86, 91,
 93
 frequency, 68
 Heisenberg, 27, 42–43, 45, 47, 50, 63, 66,
 72, 85, 86, 91, 93, 265, 256, 293
 rate, 46
 two-site, 43, 50, 59
- FepA, 252, 265–272
- Ferric enterobactin, 265, 271–272
- Field modulation, 343, 344
 amplitude (B_m), 365
 frequency (ν_m), 343
- Fluid phase, 16
- Gaussian lineshape, 7, 13
- Food stability, 339–341, 355, 359; *see also*
 Stability
- Free radicals, 378
 biodistribution and measurement in vivo,
 378
 drug intermediate, 381
- Free spin test, 297, 298
- Free volume: *see* Volume
- Freeze concentrated solution, 348, 349, 365

- Freeze pump-thaw, 93, 94
 Fructose, 351
- g*-factor shift, 97
 tensor, 341, 343
- Gas permeable capillary, 94
- Gel phase, 16, 97
 interdigitated, 75
 membranes, 62–64, 73
- Gene-32 protein, 327–328
- Glass, 343, 348–353, 356
 carbohydrate-water, 351
 glucose-water, 354
 maltodextrin-water, 355
 maltoheptaose-water, 352
 specific transition temperature (T_g'), 348, 349
 sucrose-water, 350
 sugar-water, 348, 353, 365
 transition (T_g), 349–354, 355, 360
- Glass-rubber transition, 339, 349, 355
- Gliadin, 356, 357
- Glucose, 351, 353–356
- Glutathione
 ESR detection, 152, 153
 intracellular, 155, 156
 spin labeled, 132, 141
- Gluten, 356–360
 maleimide spin labeled, 341, 356–360
- Glutenin, 356
- Glycerol, 345, 346, 354, 361–365
 glycerol water, 345, 361, 364, 365
- Heisenberg spin exchange, 27, 42–43, 45, 47,
 50, 63, 66, 72, 85, 86, 91, 93, 265,
 256, 293
- α -helix, 259–260, 274
 in gluten, 358
- Hemagglutinin, 276–277
- Hemoglobin, 159
 spin labeled, 32, 34, 365
- High-field ratio: *see* Line height ratio
- Homogenous broadening, 53
- Human growth hormone, recombinant, 104–
 105
- Human serum albumin
 electrostatic potential, 147–148, 159
 reaction with disulfide biradicals, 155
 spin-labeled, 147–149, 159
- Hybridization, 320–323, 334
- Hydrodynamic theory, 345
- Hydrodynamic volume, 34–36; *see also* Volume
- Hydrogen bond, 340, 346–348, 353, 356, 358, 360
 network, 354
- Hydroxylamine, 127
- Hydroxy-TEMPO, (TEMPOL), 31, 33, 35–36,
 340–341, 376
 ^{15}N derivative, 31–35
- Hyperfine, 83–105
 anisotropy, 406
 coupling, 192
 deuterium, 85
 interaction, 192
 isotropic, 406
 principal axes, 196
 tensor, 196
- Ice, 350
 crystallization, 348, 349
 crystals, 351
 formation, 354
 melting, 349–352
- Imidazolidine nitroxides, 113, 122, 125, 127,
 140, 141, 145, 150, 174, 175; *see*
also Imidazoline nitroxides
- Imidazoline nitroxides
 pK, 114–122, 127–129, 140, 142–143
 protonation, functional groups, 113, 122
 spin-labeling reagents, 140
- 2-Imidazoline-3-oxides, 175; *see also* Nitronyl
 nitroxides
- Inhomogeneous broadening, 6, 9, 14, 16,
 54–55, 85, 90, 93
- Interaction parameter (k), 344, 347, 350, 362
- Interactions
 ligand–protein, 271–272
 peptide–membrane, 273–278
- In vivo EPR, 367–404
 rationale, 368
 potential constraints, 371
 sensitivity considerations, 375
 pH measurement, 134, 135
 spin trapping, 382
- Iodoacetamide nitroxide, 140, 340
- Isothiocyanate nitroxide, 140, 340
- Isotropic hyperfine coupling, 406
- K**, interaction parameter, 344, 347, 350, 362
- Kaolin, pH in mesopores, 130, 131
- Lac permease, 271–272
- β -lactamase, 243
- L-band EPR, 375–376

- Lever rule, 17
- Line height ratio
 center-field ratio C'/C , 364
 high-field ratio H''/H , 359, 364
 low-field ratio L''/L , 354, 355, 362–365
 R parameter (h_i/h_m), 357
- Ligand–protein interaction, 271–272
- Linewidth parameters, 84, 85, 87, 91
- Lineshape, Lorentzian, 6, 9, 13
- Lipid
 bilayer, 16, 42, 73
 exchange, 59
 phase diagram, 17
 protein interactions, 59, 62
 spin label, 33, 59, 63, 69, 405
 translational diffusion, 63
- Lipopolysaccharide, 173
- Liposomes
 nitronylnitroxide incorporation, 169, 171
 pH in the inner volume, 132
 transmembrane transport, 138, 139
- Liver alcohol dehydrogenase, 243
- Loop-gap resonator, 252, 321
- Lorentzian lineshape, 6, 9, 13
- Lysine labeling, 104–105
- T4 lysozyme, 273
- M13 bacteriophage coat protein, 71
- MAL-6, 254
 spin labeling, 253
- Maleimide spin label (MSL), 2,2,6,6-tetra-
 methyl-4-maleimidopiperidine-1-oxyl,
 34, 77, 102–103, 253–254, 341
- Maltodextrin, 355, 356
- Maltoheptaose, 352, 353
- Malto-oligosaccharide, 351
- Maltopentaose, 352
- Maltose, 351
- Maltotriose, 352
- McConnell, Harden, 1–2
- Melittin, 277–278
- Melting temperature (T_m), 354, 360
 special (T_m'), 351, 352, 360
- Membrane, 59, 64, 66, 405
 gel phase, 62–64, 73
- Membrane depth, 257–258
- Membrane proteins, 251–259
 bacteriorhodopsin, 258, 259–260
 FepA, 252, 265–272
 lac permease, 272–273
 rhodopsin, 260–264
- Metal ions, measurement in tissues, 377
- N-methoxy-N-nitrosoamines, 68
- S-Methyl-2-nitrosopropane (MNP), spin trap-
 ping, 91, 295–297, 382
- Microscopic ordering, 99
- Microwave power saturation, 299
 cavity, 365
- Microwave radiation
 field strength (B_1), 365
 frequency, 343
 X-band, 343
- MNP (S-methyl-2-nitrosopropane)
 spin trapping, 91, 295–297, 382
- Mobility, *see* motion
- Modulation, field
 amplitude, 361, 363, 365
 Zeeman, 58
 frequency, 343, 363
 Zeeman, 56, 58
- Molecular distances, 104
- Molecular dynamics (MD), 304, 330, 332
- Molecular modeling, 206, 223
- Motion
 isotropic, 341, 342, 364
 molecular, 341, 344, 349, 353
 rotational, 341, 352
 sensitivity for, 343, 355, 363
- Motional region
 fast, 342
 slow, 343
 very slow, 343
- MSL (2,2,6,6-tetramethyl-4-
 maleimidopiperidine-1-oxyl), male-
 imide spin label, 34, 77, 102–103,
 253–254, 341
- MTSL, 1-oxyl-2,2,5,5-tetramethylpyrroline-3-
 methylmethanethiosulfonate,
 244–245, 253–255
- Multilamellar vesicles, 96
- Myelin proteolipid protein, 59–60
- Na^+K^+ -ATPase, 65
- Ni^{2+} ions, paramagnetic relaxant, 71, 76
- N-methoxy-N-nitrosoamines, 68
- Nitric oxide, *see also* NO
 donors, 168
 ESR detection, 162
 reaction with nitronylnitroxides, 162–168
 synthase, 169, 171, 172
- N^{10} -monomethyl-L-arginine, 172, 174
- N^{10} -nitro-L-arginine, 172, 174

- Nitronyl nitroxides
 histidine analog, 123
 incorporated protonation, 112
 NO liposome, 168–172
 reaction with NO, 162–168, 172
 spin-labeled angiotensin, 141
- Nitroprusside, 168
- Nitroxide, *see also* spin label
 alkylating, 141, 147
 amidino, 140
 amino, 122, 140
 3-amino-PROXYL, 289, 290
 4-amino-TEMPO, 289, 290, 321, 323
 azido, 140
 bioreduction, 373
 carbodiimide spin label, 77, 140
 enaminketone, 128
 imaging, 390
 iodoacetamide, 140, 340
 isothiocyanate, 140, 340
 5-membered ring, 285–289
 6-membered ring, 285–289
 metabolism, 378
 MSL (2,2,6,6-tetramethyl-4-maleimidopiperidine-1-oxyl), maleimide spin label, 34, 77, 102–103, 253–254, 341
 MTSL (1-oxyl-2,2,5,5-tetramethylpyrroline-3-methylmethanethiosulfonate), 244–245, 253–255
 pH sensitive nitroxides, 384
 pharmacokinetics, 391
 succinimido, 140
 SSL (succinimidyl-2,2,5,5-tetramethyl-3-pyrroline-1-oxyl-3-carboxylate), 104, 105
 TEMPO (2,2,6,6-tetramethyl-piperidine-1-oxyl), 95–97, 356
 TEMPOL (Hydroxy-TEMPO, TANOL), 31, 33, 35–36, 340–341, 340, 345, 346, 350–356, 361, 365, 376
¹⁵N derivative, 31–35
 TEMPONE (2,2,6,6-tetramethyl-piperidone-1-nitroxide), 32, 85–87, 94
 S-Nitroso-N-acetylpenicillamine (SNAP), 172
 NMR, 341
 NO, *see also* Nitric oxide
 donors, 168
 ESR detection, 162
 reaction with nitronyl nitroxides, 162–168
 synthase, 169, 171, 172
 Nuclear relaxation, 26, 37, 39, 50
 mechanisms, 35
- Oligonucleotides, spin labeled chemical synthesis, 284, 287–291, 299, 334
- Oligosaccharide, 351, 352
- OmpA, presequence, 21
- Order parameter, 314, 315, 318, 405
 tensor, 406
- Oxygen
 measurement in tissues, 377, 385
 paramagnetic relaxant, 40, 69
 particulate paramagnetic materials for measuring, 380
 in tumors, 388
- 5-[(1-Oxyl-2,2,5,5-tetramethyl-3-pyrrolidiny)amino]-2'-deoxyuridine (DUPDA), 285, 289
- 5-[(1-Oxyl-2,2,6,6-tetramethyl-4-piperidiny)amino]-2'-deoxyuridine (DUTA), 285, 288, 289, 292
- Π , accessibility parameter
 definition, 261
 periodicity, 267, 268, 274
- Φ -values, 257–267
 definition, 257–259
 depth, 257–258
 for FepA mutants, 258, 267–268
 for lipids, 258
- $P_{1/2}$, definition, 256
- Papain, 243
- Paramagnetic relaxant
 chromium oxalate, 69
 ions, 40
 Ni²⁺ ions, 71, 76
 oxygen, 40, 69
- Partitioning, 96
- PBN, Phenyl-*tert*-butylnitron, 91, 92
- PD-TEMPONE (perdeuterated 2,2,6,6-tetramethyl-4-piperidone-1-oxyl), 86–88, 93
- Peptide-membrane interactions, 273–278
- Peptides
 alamethicin, 276
 cecropins, 274–276
 diphtheria toxin, 273–274
 hemagglutinin, 276–277
 melittin, 277–278
- Periodicity, 268
- PGSL phosphatidyl glycerol spin label, 67–71
- pH measurement
 in cross-linked polyelectrolytes, 130
 in kaolin, 130, 131
 in phospholipid vesicles, 132

- pH measurement (*cont.*)
 in tissues, 377
 in vivo, 134, 135
 in water-in-oil systems, 131
 in zeolites, 130, 131
- pH sensitive nitroxides, 384
 biradicals, 124, 125
 iminonitroxides, 112
 nitronylnitroxides, 112, 122
 spin labeling reagents, 140
 triradicals, 125
- Pharmacokinetics, 378, 391–392
- Phase diagram, lipid, 17
- Phase separation, 365
- Phase transition, 97, 98, 100
- Phenyl-*tert*-butylnitron (PBN), 91, 92
- Phenyl radical, 91, 92
- Phosphatidylcholine, 134, 143, 169
- Phospholipid, 94, 95
- Phospholipid membranes
 electrostatic potential, 138–139, 143–146
 intraliposomal pH, 132
 surface potential, 143–146
 transmembrane potential, 138, 139
 transmembrane transport, 137–140
- Phosphoramidite chemistry, 288, 291, 295–296
- Phosphotriester chemistry, 288–291
- Plasticizer, 355
- POBN, α -(4-pyridyl-1-oxide)-*N*-*tert*-butyl nitron, 172
- Point-dipole
 approximation, 196
 dihedral angle, 217
 β -lactam group, 224
- Point of connectivity, 17
- Poisson distribution
 inhomogeneous broadening, 7
 spin label population, 11
- Polarity, 97, 103
- Powder pattern, 88, 406
- PreOmpA, 21
- Protein, wheat, 356
- Proton exchange
 isotopic effect, 130
 pK for nitroxides, 112, 114–122, 125, 127–129, 140, 142–147
 rate constants, 111, 129
 titration curve, 111, 115, 135, 144, 145
- Proton transport
 in aqueous glycerol, 135–137
 across phospholipid membrane, 137, 138
- Purification, spin-labeled oligonucleotides, 292, 295–296,
- Pulsed EPR, in vivo studies, 395
- α -(4-pyridyl-1-oxide)-*N*-*tert*-butyl nitron (POBN), 172
- Reactive intermediates, in tissues, 377
- Recombinant human growth hormone, 104–105
- Relaxation agents, 251, 255, 257
- Relaxation
 dipolar, 40, 72
 enhancement, paramagnetic, 37, 69, 72
 nuclear, 26, 37, 39, 50
 time, effective spin lattice (T_1), 26, 37, 45, 47, 50, 343, 344, 355, 364
- Resolution, EPR spectra, 90, 97
- Rheological studies, 358, 360
- Rhodopsin, 252, 260–264
- Rigid limit, spectra, 88, 97
- Ripple phase, 97
- Rotational correlation time, 29, 33, 35, 78, 341–344, 349, 350, 355–359, 361, 365
 calibrations, 78
 isotropic, 341
- Rotational diffusion, 29, 77
- Rozantsev, Eduard, 2–4
- Rubbery state, 349
- Sample deoxygenation, CW HF EPR experiments, 93–95
- Saturation, 24, 45, 52, 343, 365
 CW, 25, 52, 255–256
 first derivative, 53, 55
 integrated intensity, 53, 55
 parameter, 52
 progressive, 55ff, 59, 68, 70–71
 recovery, 272, 344
 transfer, 343, 365
- Saturation transfer EPR, *see* ST-ESR
- SDSL (site-directed spin labeling), 251–252
 depth, 257–258
 membrane proteins, 259
- Simulation, 304, 306, 314, 316, 330, 331
- Site-directed spin labeling (SDSL), 251–252
 depth, 257–258
 membrane proteins, 259
- Slip, 345, 360
- Slow motional effects, 86, 90, 102, 105, 405, 407
- Slowly relaxing local structure (SRLS), 304, 305, 318

- S-Methyl-2-nitrosopropane (MNP), spin trapping, 91, 295–297, 382
- S-Nitroso-N-acetylpenicillamine (SNAP), 172
- Spectral densities, 28, 40, 84, 85, 91, 93
- Spin label, 339–342, 348, 356
- accessibility, 255
 - carbodiimide, 77
 - CTPO, 33
 - deuteriated, 185
 - fast limit values, 306
 - g** tensors, 302–303, 307, 310
 - immobile, 357, 359
 - lipid, 33, 59, 63, 69, 405
 - mobile, 357
 - molecular shape, 345–346
 - molecular structure, 185
 - motion, 253
 - oxypyrrolinyl, 185
 - rigid-limit tensors, 302
 - A** tensors, 302–303, 307, 310
 - SSL (succinimidyl 2,2,5,5-tetramethyl-3-pyrroline-1-oxyl-3-carboxylate), 104, 105; *see also* Nitroxide
 - sulfonic acid, 132, 138
 - triple spectroscopy, 201
- Spin labeled
- 26-mer, 293–296, 301, 329, 331, 333
 - g** tensors, 302–303, 307, 310
 - amino acids, 211
 - deoxycytidine analog
 - DCAT, 286, 323, 324
 - DCAVAP, 287, 295
 - fatty acid, 97–102
 - methane thiol-sulfonate, 244
 - methylalanate, 184, 211–215
 - methyl tryptophanate, 215, 218–219
 - oligonucleotides, 284, 287–288, 290–292, 294
 - chemical synthesis, 284, 287–291, 299, 334
 - enzymatic synthesis, 284, 292, 299
 - penicillin, 208–209, 221, 233
 - phenylalanine, 219, 220
 - proteins, 82–105
 - thymidine analogs, 285–287, 293
 - ACET, 285, 302–304
 - DUAP, 286, 294, 296, 301, 303, 310, 314–318, 323, 326, 327, 330
 - DUAT, 286, 293, 294, 301, 303
 - DUAVAP, 287, 293, 294
 - DUMPDA, 285, 289, 290, 298, 301, 321, 322
 - DUMTA, 285, 290, 298, 303, 315, 316
 - DUPA, 286, 293
- Spin labeling
- cysteine, 253
 - double cysteines, 263–265
 - with MAL-6, 253
 - membrane proteins, 259–273
 - with MTSL, 253
 - sequence-specific, 284, 293–294, 296, 299
 - site-directed, 251, 252
- Spin pH probes, 110, 115, 130, 132, 140
- Spin–spin interactions, 11
- Spin trapping, 91, 382, 295
- C5-iodo-deoxyuridine, 295
 - in vivo EPR, 382
 - 2-methyl-2-nitrosopropane (MNP), 295–297
 - POBN, α -(4-pyridyl-1-oxide)-N-tert-butyl nitrone, 172
- SRLS (slowly relaxing local structure), 304, 305, 318
- Stability
- food, 339, 349
 - nitroxide, 340
 - storage, 339
- Starch, 355
- State diagram, 348, 349, 353
- Statistical distribution, spin labels, 13
- ST-ESR, 56, 58, 62, 64–65, 74, 76–77, 340–343, 348, 356–359, 365
- calibration spectrum, 344, 354, 363
 - integral measuring protocol, 348–349
 - phase reference experiments, 359
 - reference spectra, 365
 - spectrum, 344, 361
- Stickiness parameter *S*, 345–347, 360
- Stokes–Einstein equation modified, 344, 345, 362
- Structure, nitroxide spin labels, 341
- Succinimido nitroxide, 140
- Succinimidyl-2,2,5,5-tetramethyl-3-pyrroline-1-oxyl-3-carboxylate (SSL), 104, 105
- Sucrose, 347–351
- Sugar, 339–341, 348–354, 361, 364, 365
- Sulfonic acid spin label, 132, 138
- Superhyperfine, 88, 89
- Superoxide radical, reaction with thiols, 158
- T_1 ; *see* Spin-lattice relaxation time
- TEMPO, (2,2,6,6-tetramethyl-piperidine-1-oxyl), 33, 95, 96, 97, 356
- TEMPOL (Hydroxy-TEMPO), 31, 33, 35–36, 340–341, 340, 345, 346, 350–356, 361, 365, 376
- ^{15}N derivative, 31–35

- TEMPONE (2,2,6,6-tetramethyl-4-piperidone-1-nitroxide), 32, 63, 85, 86, 87, 94
- Tensor: *see* A tensor; g tensor
- TEPOPL,O-[3-(2,2,5,5-tetramethyl-1-oxypyrrolinyl)-propen-2-oyl]-L-β-phenyllactate, 237-240
- 2,2,5,5-tetramethyl-1-oxypyrrolinyl-3-carbonyl)-L-alanate (methyl-L-alanate spin label), 184-186, 192-193, 195, 198-201
- 2,2,5,5-tetramethyl-1-oxypyrrolinyl-3-carboxylic acid, 201-206
- 4-(2,2,5,5-tetramethyl-1-oxypyrrolinyl-3-carbonyl)-L-phenylalaninal, 231-237
- 3-(2,2,5,5-tetramethyl-1-oxypyrrolinyl)-2,4-pentadienal, 225-227
- 3-(2,2,5,5-tetramethyl-1-oxypyrrolinyl)-2,4-pentadienoic acid, 225-228
- 3-(2,2,5,5-tetramethyl-1-oxypyrrolinyl)-2-propenamide, 207
- Thiocholine, 158
- Thioglycerol, 113, 169-170
- Thiols
- in the blood, 156
 - ESR detection, 149, 155-157
 - in isolated organs, 156-157
- Thiols(*cont.*)
- spin-labeling SH-groups, 159
 - thiol-disulfide exchange, 149, 150
- Translational diffusion, lipids, 63
- Trehalose, 351
- Trichloromethyl radical, 91, 92
- Triradicals, 123, 125
- Valinomycin, 139
- Van der Waals volume: *see* Volume
- VAR (very anisotropic reorientation) model, 407
- Varian E-104, 298-301
- Very anisotropic reorientation (VAR) model, 407
- Viscosity, 344, 349, 350, 362
- Voigt lineshape, 7, 13
- Volume
- free, 353, 356, 360
 - hydrodynamic, 346
 - Van der Waals, 345
- W-band EPR, 83-107
- Williams-Landel-Ferry (WLF) equation, 362
- X-band EPR: *see* Microwave radiation
- Zeolites, pH in mesopores, 130, 131